Heritage Science

RESEARCH

Open Access

Experimental study on weathering mechanism of ancient bricks in Jiayuguan Wei-Jin tombs, Gansu, China

Lihong An[1,2], Zhen Qiao[3,4*], Jie Wang[3,4] and Fengrui Wang[3,4]

Abstract

This study focuses on the ancient bricks of Wei-Jin tombs in Jiayuguan, Gansu, China, analyzing the deterioration of the bricks under the long-term influence of natural environments and human activities. Currently, the ancient bricks exhibit various degradation diseases such as cracks, exfoliation, fracture, weathering, and microbial erosion, severely affecting the integrity of the cultural relics. Through on-site investigation and characterization testing, the physical and mechanical properties, compositional elements, pore size distribution, and thermal characteristics of the ancient bricks were analyzed. Indoor simulation experiments were conducted to study the impact of different types of environmental erosion cycles (such as H_2O, HCl, NaOH, Na_2SO_4) on the performance and structure of the ancient bricks, the patterns and causes of deterioration were also studied. The results indicate that the cyclic effects gradually transform the porosity of the ancient bricks into lateral microcracks, which continue to expand, leading to varying degrees of degradation of performance. The extent of the impact of these cycles on the properties of ancient bricks is in descending order: Na_2SO_4, HCl, NaOH, H_2O. H_2O, NaOH, HCl, Na_2SO_4.

Keywords Tombs, Ancient bricks, Cyclic effects, Deterioration

Introduction

The Jiayuguan Wei-Jin Tombs located in Jiayuguan, Gansu province, China, which were rightfully recognized and included in the fifth group (2001) of the National Key Cultural Relics Protection Units in China. The ancient tombs playing a vital role in the study of Wei-Jin culture. The Wei-Jin tombs have a unique structural design, the tomb chamber structure was entirely stacked with bricks without any adhesive materials, typically comprising two or three tomb chambers. The ancient bricks in tombs have deteriorated in properties due to long term external influences, which posing a threat to the integrity of the tomb structure, thus urgently necessitating protective measures [1, 2].

In recent years, extensive studies were conducted on the impact of cyclic effects on the properties of ancient bricks. The effects of freeze–thaw cycles on the performance and structure of ancient bricks were studied, indicating that freeze–thaw cycles significantly impact the performance of ancient bricks, with the internal pores gradually becoming interconnected, ultimately leading to the destruction of the brick structure [3–5]. The patterns of structural damage and deterioration of ancient bricks under the influence of load and environmental factors was studied, and the results showed that the application of load accelerates the destruction of ancient bricks under freeze–thaw conditions, and the combined effect

*Correspondence:
Zhen Qiao
409434721@qq.com
[1] Jiayuguan Great Wall Museum, Jiayuguan 735100, China
[2] Jiayuguan Silk Road (Great Wall) Cultural Research Institute, Jiayuguan 735100, China
[3] Northwest Research Institute Co., Ltd., China Railway Engineering Corporation, Lanzhou 735100, China
[4] Key Scientific Research Base of Conservation for Heritage Building of Bricks and Stones, Cultural Heritage Bureau of Gansu Province, Lanzhou 735100, China

of load and sodium sulfate is even more significant in causing damage [6, 7]. Some scholars demonstrated that ancient bricks from different regions, due to variations in their hygroscopic abilities, exhibit different rates of performance deterioration, and collectively highlight the complexity and variability of factors affecting the durability and integrity of ancient bricks, underscoring the need for region-specific and condition-specific conservation strategies [8–10].

Salt damage to cultural relics is a common phenomenon, especially in arid areas along the Silk Road, where this effect is more seriously. Some researchers found that soluble salts are the primary cause of material deterioration, structural damage, and strength loss in the brick materials of the ancient masonry [11, 12]. The relationship between crystalline height and solubility was studied, which affected by salt type and crystallinity [13]. The distribution of salt in the masonry also depends on the mixing degree of salts and their sources, sulfates are mainly enriched on the surface and nitrate only crystallize in small amounts [14]. Deposition and mechanism of sodium chloride in marine environment was also studied by other scholars [15, 16]. However, the research of cyclic soluble salts effect on the properties of ancient masonry was barely reported, further study is needed on the weathering and damage of ancient bricks caused by the joint action of the erosive environment and daily meteorological data changes during precipitation.

According to preliminary studies, the main factors affecting the Wei-Jin tombs in Jiayuguan include temperature, humidity, and corrosive agents. To study the degradation patterns of the ancient bricks, this paper conducts simulated experiments on bricks under various types of environmental erosion cycles (such as H_2O, HCl, NaOH, Na_2SO_4), which aiming to obtain the impact of different cycles on the performance and structure of the ancient bricks. The mass, ultrasonic wave velocity (V_p), uniaxial compressive strength (UCS) and microstructure of the ancient bricks before and after cycling were measured using environmental erosion cycles with different immersion media and different cycles. The damage characteristics and damage mechanism were analyzed using scanning electron microscopy (SEM), X-ray diffraction (XRD), and mercury injection (MIP) tests. This paper provides a useful reference for the treatment of weathering diseases in the Wei-jin tombs.

Experimental section

Research background

The Wei-Jin tombs located in northeastern of Jiayuguan district, which contain seven typical tombs, and the No. 6 tomb was selected as research object. Currently, the ancient bricks exhibit various degradation diseases such as cracks, exfoliation, fracture, weathering, and microbial erosion (Fig. 1).

Although the Wei-Jin tombs in Jiayuguan are located underground, they are open to the public as a cultural heritage site and are visited by tourists throughout the year, leading to continuous fluctuations in the temperature and humidity inside the tomb chambers. The meteorological data (average monthly temperature, relative humidity, etc.) for the Jiayuguan Wei-Jin tomb from 2018

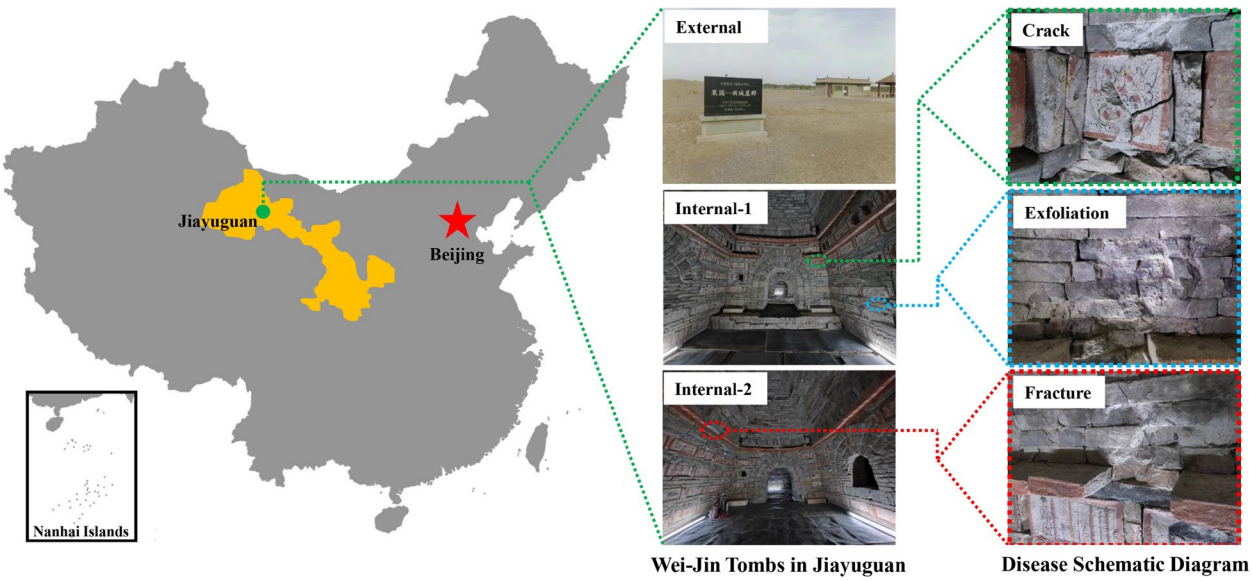

Fig. 1 Schematic images showing the deterioration of the Wei-Jin tombs in Jiayuguan

to 2020 were collected, as well as statistical data on visitor numbers. The meteorological data for the Jiayuguan Wei-Jin tomb chambers from 2018 to 2020 is shown in Fig. 2.

Disease cause analysis

Analysis from Fig. 2 indicates that there are significant fluctuations in the humidity within the tomb, ranging from RH30% to RH90%, with temperature variations between 0 and 20 °C. The temperature in the tomb remains above 0 °C throughout the year, thus the impact of freeze–thaw cycles is minimal. At the same time, samples of severely deteriorated bricks from the tomb were collected for analysis. Tests were conducted to characterize their compositional elements and pore size distribution, in order to study the influence of pore size and composition on the degradation of bricks. The XRD diffraction patterns and Fourier Transform Infrared Spectrometer (FT-IR) spectra of the ancient brick samples are shown in Fig. 3.

As shown in Fig. 3, an absorption peak near the wavenumber of 3750 cm^{-1} can be observed, corresponding to the absorption peak of the -OH group. The absorption peaks at 1473 cm^{-1} and 874 cm^{-1} correspond to the O-C-O group, and the absorption peak at 470 cm^{-1} corresponds to the characteristic absorption peak of the Si–O–Si group, indicating the presence of components such as $Ca(OH)_2$, $CaCO_3$, and SiO_2. In order to further analyze the relationship between composition and performance, the mineral composition of the brick samples was analyzed. XRD diffraction patterns show that the ancient brick samples have three intense diffraction peaks at $2\theta = 20.86°$, 26.64°, and 50.14°, corresponding to the three strong peaks of SiO_2 (PDF card number: 99–0088), indicating that the main component of the sample is quartz. Three weaker diffraction peaks at $2\theta = 29.46°$, 39.48°, and 48.61° correspond to $CaCO_3$ (PDF card number: 05–0586), indicating the presence of a certain amount of calcite in the sample. Additionally, the sample contains small amounts of gypsum, albite, and illite. The compositional analysis indicates the presence of sulfates (mainly gypsum, which does not easily leach out) in the deteriorated samples, suggesting the enrichment of sulfate in the weathered samples.

Analysis from Fig. 4 reveals that the pore size distribution of the ancient brick is mainly between 671–2465 nm, with the most prevalent pore size being 2873 nm, accounting for a pore distribution of 0.22 mg $\cdot L^{-1}$. In terms of pore length distribution, pores with a diameter of 1043 nm have the longest length, reaching 7.3×10^{-5} nm $\cdot$mg $\cdot L^{-1}$, followed by those with diameters of 833 nm and 1314 nm. The overall porosity of the ancient brick samples is 25.71%. According to literature [13], the carbonate content in raw materials affects the porosity of the fired products; higher carbonate content leads to more gas release during calcination, resulting in higher porosity. XRD analysis shows that the calcite content in the brick of Wei-Jin tomb is high, which contributes to the higher porosity of the ancient bricks.

To further obtain the distribution of other ions in the ancient bricks, the content of soluble salts in the weathered brick samples was tested.

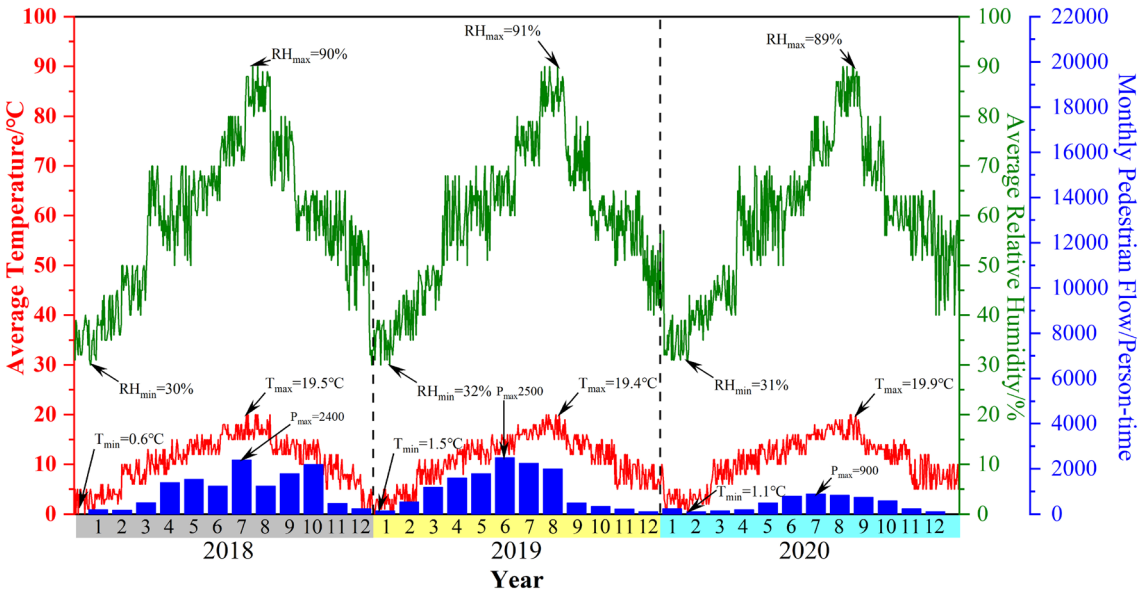

Fig. 2 The 2018–2020 climograph of the Wei-Jin tombs in Jiayuguan

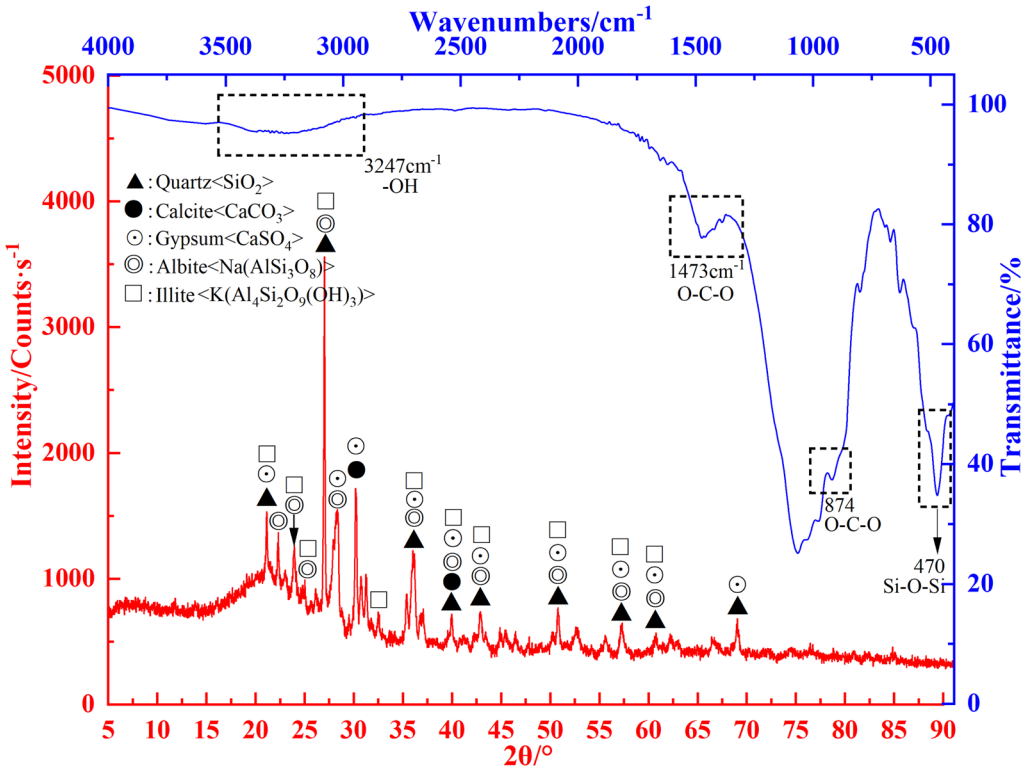

Fig. 3 XRD patterns and FT-IR spectra of samples

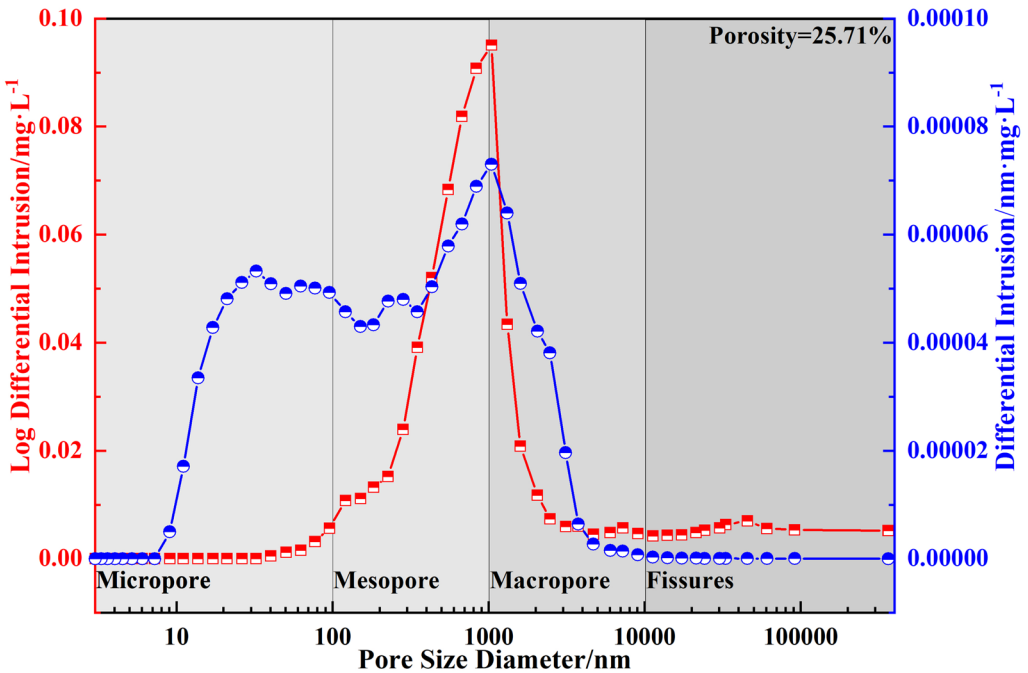

Fig. 4 MIP curves of ancient brick in Wei-jin tombs

As shown in Table 1, the ancient brick in Wei-Jin tombs enriched with various types of cations and anions, such as SO_4^{2-}, Cl^-, Na^+, K^+, so the impact of multiple ions on the properties of the ancient bricks needs to be comprehensively considered.

After preliminary investigation and study, the ancient bricks of Wei-Jin tomb own a high porosity and significant enrichment of various ions. The humidity in the tomb chamber fluctuates widely, and the CO_2 concentration in the microenvironment increases during tourist visits. These multiple factors lead to different degrees of deterioration in the ancient brick, with some areas developing cracks, exfoliation, or even fractures, severely affecting the integrity of the tomb chamber. Based on the above analysis, it is necessary to conduct different types of environmental erosion cycles (such as H_2O, HCl, NaOH, Na_2SO_4) to study the degradation patterns of the ancient bricks, thereby addressing the issues of conservation of ancient brick tombs.

Sample preparation and test methods

The experimental samples were taken from the Xincheng Tombs in Jiayuguan, which were collected from collapsed area by the management authority, and the related research has been approved by them.

The density and water absorption rate of ancient were measured by these steps. The bricks were placed in a 105 °C oven and dried to a constant weight M_d, After cooling, the bricks were immersed in water at 20 °C for 24 h, taken out and wiped dry with a towel, immediately weighed as M_s [17]. And the total volume of ancient brick (V_t) was measured by wax-sealing method. The density and water absorption rate were calculated by Eqs. (1) and (2):

$$\text{Density} = \frac{M_d}{V_t} \tag{1}$$

$$\text{Water absorption rate} = \frac{M_s - M_d}{M_d} \times 100\% \tag{2}$$

The ultrasonic wave velocity values of the samples were obtained by an RSM-SY5 (T) nonmetal acoustic detector, and were conducted on samples with diameter of 50 mm and a height of 50 mm.

The uniaxial compressive strength of the specimens was tested on a universal mechanical testing machine. The UCS tests were conducted on samples with diameter of 50 mm and a height of 50 mm. The rate of loading was 2 mm/min. All test results are the average value of three replicate samples.

Brazilian disc tests were used to test the tensile strength of samples, and conducted on samples with diameter of 50 mm and a height of 50 mm.

The basic physical and mechanical parameters of the ancient bricks are shown in Table 2, and the Thermogravimetric-Differential Scanning Calorimetry (TG-DSC) curve is shown in the Fig. 5.

Samples with obvious defects were removed, and then a nonmetal acoustic detector was used to select 10 samples for the determination of initial physical and mechanical parameters. The density of the ancient brick is about 1.74 g/cm^3, and the water absorption rate of the ancient brick is 15.21%. The Vp of ancient is about 1500 m/s, and the UCS and tensile strength are 8.42 MPa and 1.05 MPa.

As shown in Fig. 5, the weight loss in the 100–500 °C range in the ancient brick is mainly due to the disappearance of bound water, with a peak transformation point at 137.6 °C and a mass loss rate of 0.47%. The weight loss in the 500–900 °C range is mainly due to the decomposition of calcite ($CaCO_3$), with a peak transformation point at 591.2 °C and a mass loss rate of 0.87%. The weight loss in the 900–1200 °C range is mainly due to the decomposition of other minerals in smaller quantities, with a mass loss rate of 0.54%, and the phase transformation belong to the amorphous silica, which indicating that the firing temperature of ancient brick is less than 1200 °C [18].

In order to evaluate the weather resistance of the ancient bricks in Wei-Jin tombs, various groups of environmental erosion cycles tests were conducted. The sample size for this experiment was a cylinder with a diameter of 50mm and height of 50mm (height-to-diameter ratio: 1:1), as shown in Fig. 6.

Table 2 Physical and mechanical parameters of samples

Sample	Dry Density/g cm^{-3}	Water Absorption Rate/%	Ultrasonic Wave Velocity/m s^{-1}	Uniaxial Compressive Strength/MPa	Tensile Strength/MPa
Wei-Jin Tombs	1.74	15.21	1500	8.42	1.05

Table 1 Soluble salt contents of Wei-Jin tombs

Sample	Cation/mg L^{-1}				Anion/mg L^{-1}			
	Li^+	K^+	Ca^{2+}	Na^+	F^-	Cl^-	Br^-	SO_4^{2-}
Wei-Jin Tombs	27.66	164.31	221.27	194.84	44.84	229.29	31.77	302.19

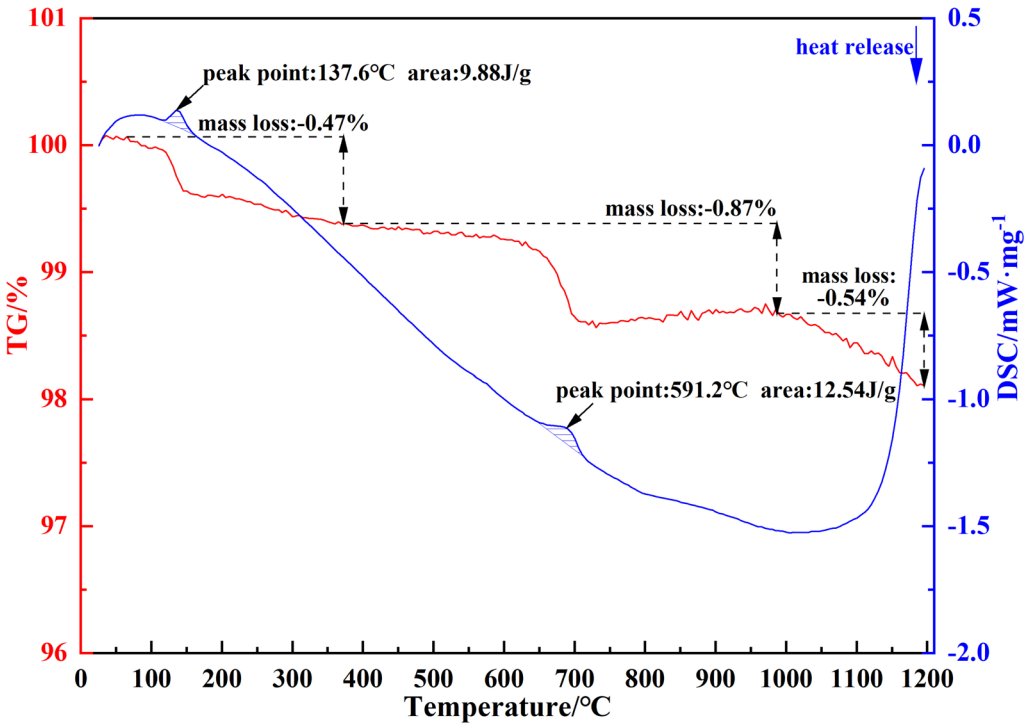

Fig. 5 TG-DSC curves of sample

Fig. 6 Digital graph of cyclic test samples

Preliminary investigations and research indicate that the ancient bricks are mainly affected by environmental erosion cycles involving water, acid, alkali, and salt. This paper characterizes and analyzes the compressive strength, ultrasonic wave velocity, mass, appearance, and microstructure of the samples during the environmental erosion cycles, thus obtaining the degradation patterns of the ancient bricks.

The collected brick samples were dried before starting the cyclic tests. The medium for the environmental erosion cycles included four types: water, acid, alkali, and salt. Each cycle consisted of a soaking process and a drying process. Based on preliminary findings, the concentrations of the media for this cycle test were set as follows: H_2O (pH approximately 6.8), 0.1 mol/L HCl solution (pH approximately 1.0), 1.00 wt% NaOH solution (pH approximately 12.4), and 10 wt% Na_2SO_4 solution (pH approximately 7.0).

Before the cycles, the samples were placed to the box which filled with 4 different media (H_2O, HCl, NaOH and Na_2SO_4) for 24 h to ensure sufficient contact with the solution. After the immersing process, the specimens were placed in the test box for environmental erosion cycles (24h), with 1 test cycle. The fast temperature

and humidity variation test box (BG/TH-100, Shanghai Bogong Equipment Co., Ltd.) was used to simulate the temperature and humidity changes in the tomb chamber which collected by monitoring instruments. Combined with temperature monitoring data in the tomb chamber, the test temperatures in the cycle were in the range of 10- 50 ℃, and the relative humidities were in the range of 30- 90%. The cyclic process contains 4 steps, which named as S1, S2, S3 and S4. As shown in Fig. 7, during S1 step, the temperature increased from 10 ℃ to 50 ℃ and the relative humidity decreased from 90 to 30% in 2 h; during S2 step, the temperature and relative humidity keep constant for 10 h; during S3 step, the temperature decreased from 50 ℃ to 10 ℃ and the relative humidity increased from 30 to 90% in 2 h; during S4 step, the temperature and relative humidity keep constant for 10 h. The Vp, UCS and mass of the bricks were tested after various cycles (5th, 10th, 15th, 20th, 25th and 30th). The appearance of the samples was recorded from 0 to 30th cycles, and the micrographs were obtained at the 5th, 10th, 15th, 20th, 25th and 30th. The XRD, SEM and MIP of specimens were tested after the 30th cycle.

The unconfined compression tester model is CXYAW-300S, produced by Zhejiang Chenxin Machinery Equipment Co., Ltd., the ultrasonic testing instrument model is RSM-SY5(T), from Wuhan Zhongke Zhichuang Geotechnical Technology Co., Ltd., the portable digital video microscope model is 3R-PPMC60-L, by Ainite Digital Technology Co., Ltd.. The X-Ray Diffraction (XRD) instrument model is D/MAX-2400, by Rigaku Corporation, Japan. The Scanning Electron Microscope (SEM) model is S-4800, by Hitachi Ltd., Japan. The FT-IR model is Tensor 27, by Bruker Corporation, Germany. The Mercury Intrusion Porosimeter model is MicroActive AutoPore, by Micromeritics Instrument (Shanghai) Co., Ltd. The Thermogravimetric Analyzer model is DSC-1/700, by Mettler-Toledo, Switzerland.

Result and discussion

Deterioration characteristics

Minerals composition changes

After the environmental erosion cycles, the XRD test of each group was tested, and the results are showed in Fig. 8. Qualitative analysis of the mineral composition and its relative content was performed using XRD data. As Fig. 8 shown, after the cycles, there was a change in the relative content of mineral compositions. This change was primarily characterized by an increase in the quartz and clay minerals content, while the contents of calcite and albite decreased. The mineral content of the brick in four different medium environments has the same variation rule, but the variation amplitude is different to some extent. Among them, the relative content of minerals in Na_2SO_4 solution changed most obviously,

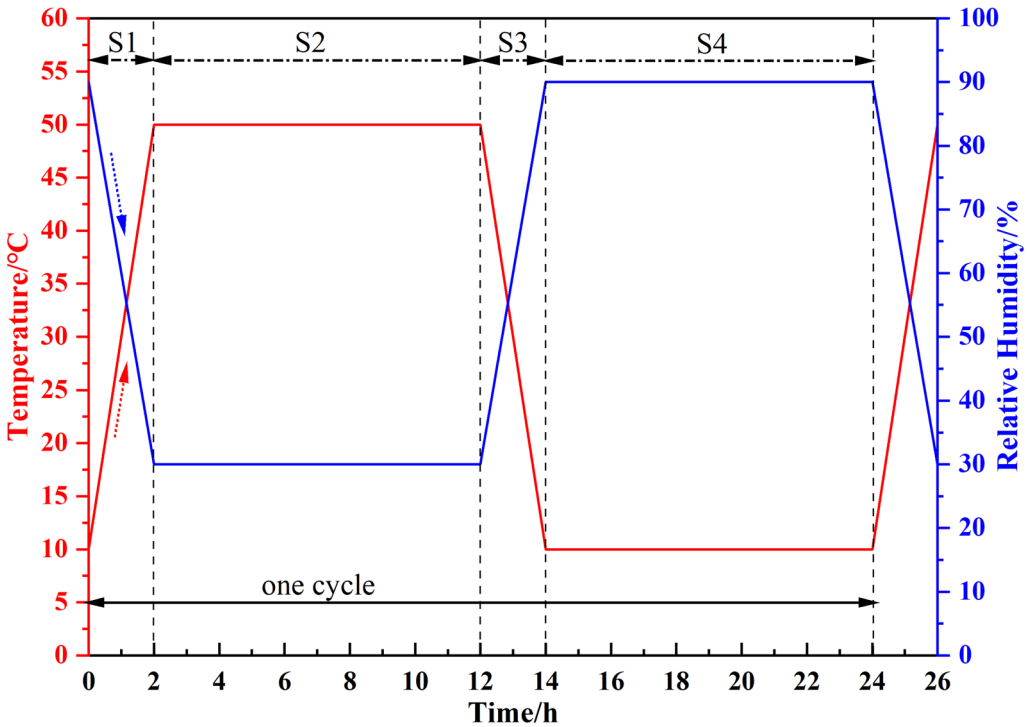

Fig. 7 Schematic diagram of the temperature and humidity change in the cycle

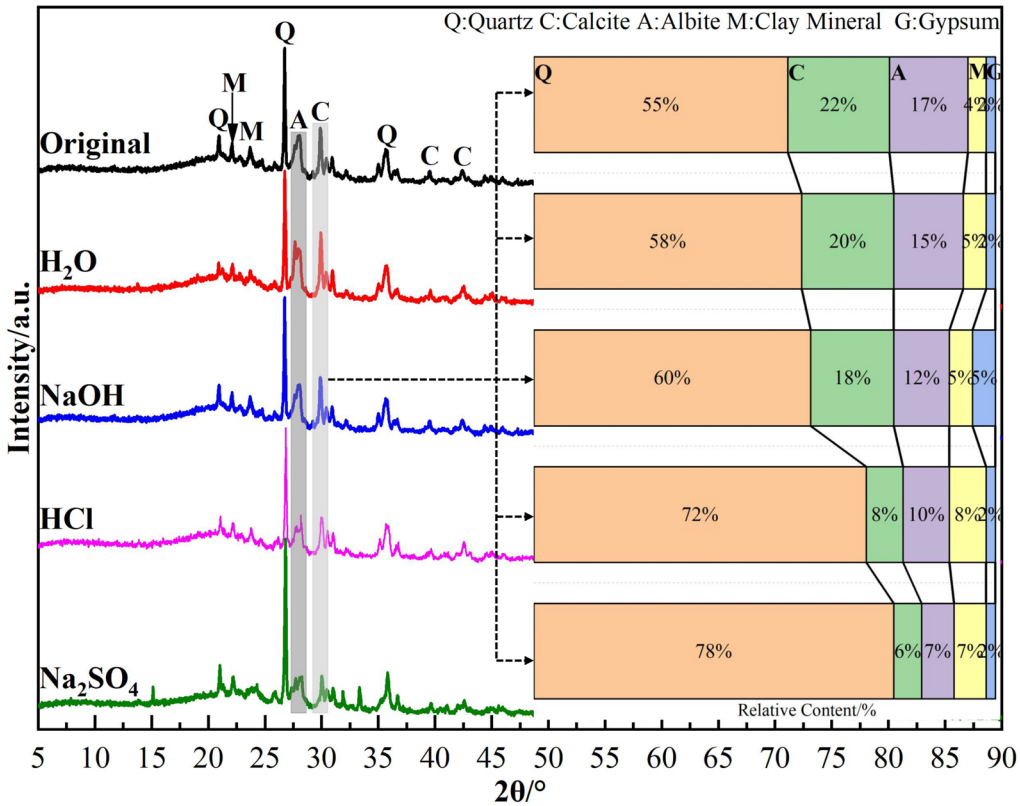

Fig. 8 XRD patterns and semi-quantitative analysis of samples after cycling

the relative content of feldspar and calcite decreased by 10.0% and 16.0%, and the relative content of quartz increased significantly by 23.0%. The relative mineral contents in the four mediums were in the order of $Na_2SO_4 > HCl > NaOH > H_2O$.

Porosity changes

The MIP of each group after cycling were showed in Fig. 9. The pore size distribution of the ancient brick in initial state is mainly between 671 and 2465 nm, with the most prevalent pore size being 2873 nm, and the overall porosity of the ancient brick samples is 25.71%. After the environmental erosion cycles, the porosity of the sample increased in different extend. After H_2O and NaOH cycles, the pore size distribution of sample is still mainly between 675 and 3118 nm, but the porosity increased to 27.25% and 28.04%, respectively. Under HCl cycles, the pore size distribution is mainly between 826 and 3785 nm, which is bigger than initial state, and the porosity increased to 30.95%. And after Na_2SO_4 cycles, the pore size distribution changed from mesopore to macropore, the greatest number of cracks was observed, and the porosity significantly increased to 35.14%. Damage from the environmental erosion cycles was manifested in the ancient brick as an increase in the number of macropores, the development of medium and small pores.

Microstructure changes

The analysis of Fig. 10 suggests that under different t environmental erosion cyclic conditions, the size of the lamellar structure and the degree of bonding between layers of the ancient brick undergo changes. With an increasing number of cycles, fissures gradually develop, altering the overall integrity of the microscopic morphology. From the analysis of Fig. 11a, it can be seen that after the 30th H_2O cycles, the overall bonding is relatively tight, but some microcracks appear, with a width of about 1μm, and there are fewer microscopic defects in the samples. According to Fig. 11b, after the 30th HCl cycles, the microscopic morphology locally shows some irregularly shaped granular particles, and a certain number of microcracks develop, leading to a lower overall integrity. As shown in Fig. 11c, after the 30th NaOH cycles, the samples are primarily characterized by lamellar structures, with a size of about 5–10 μm, and fewer microscopic defects. Finally, Fig. 11d indicates that after the 20th Na_2SO_4 cycles, the lamellar structures observed within the field of view are about 1–3 μm in size, with a

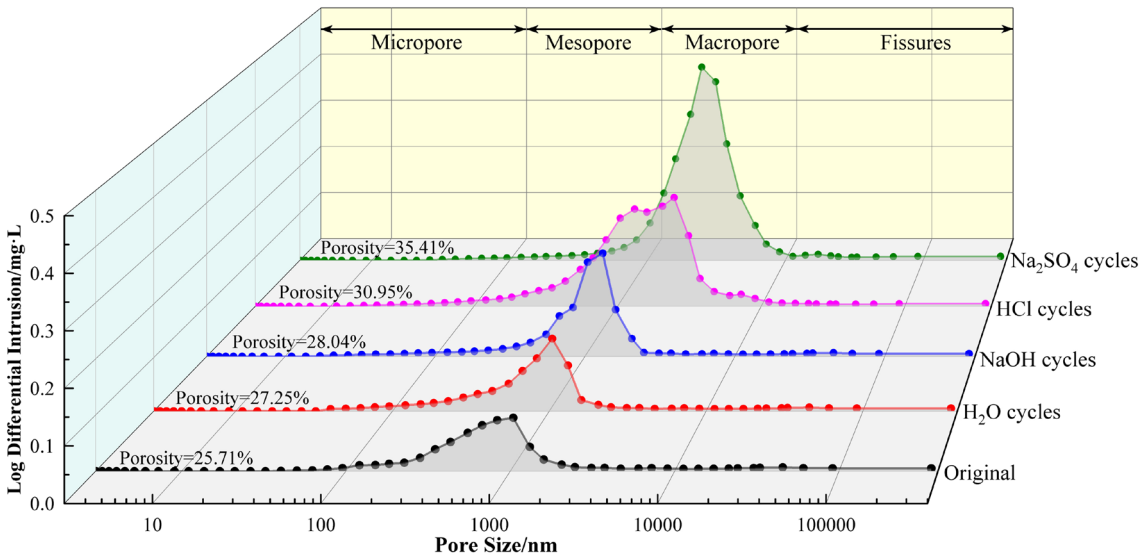

Fig. 9 MIP curves of samples after cycling

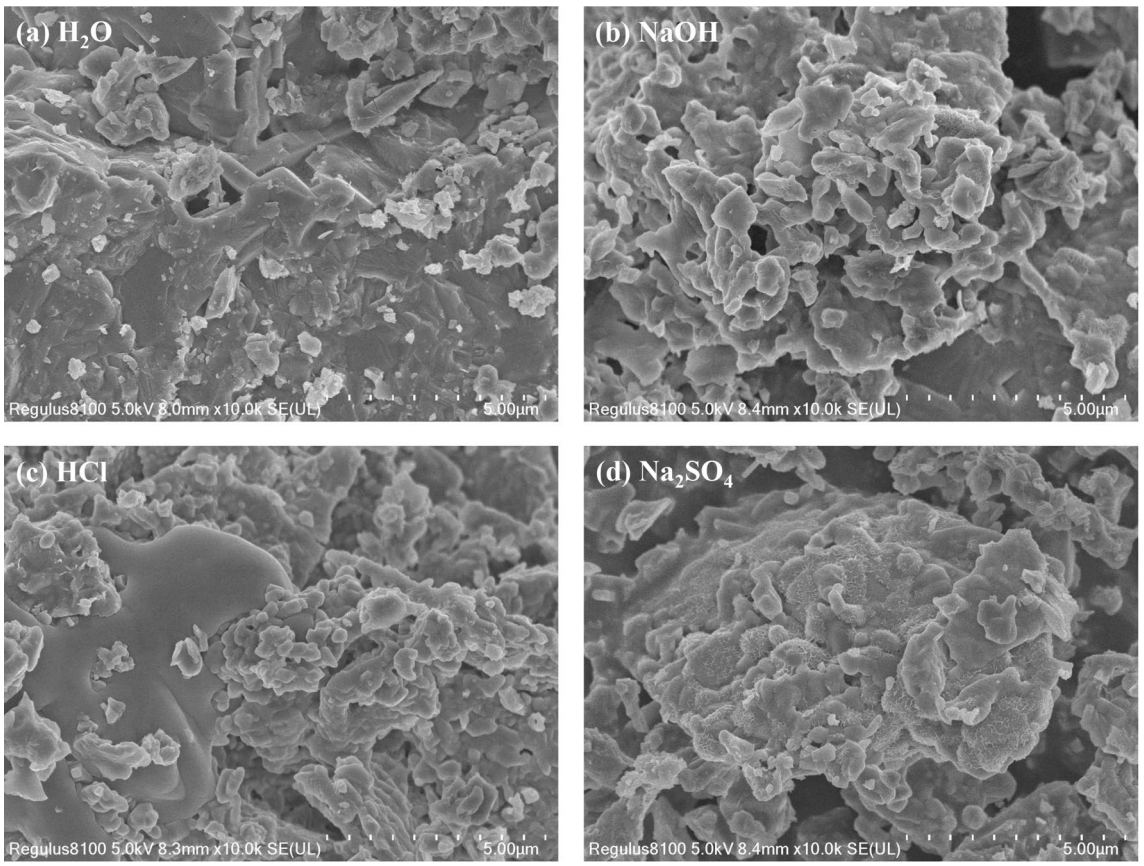

Fig. 10 SEM images of samples after cycling

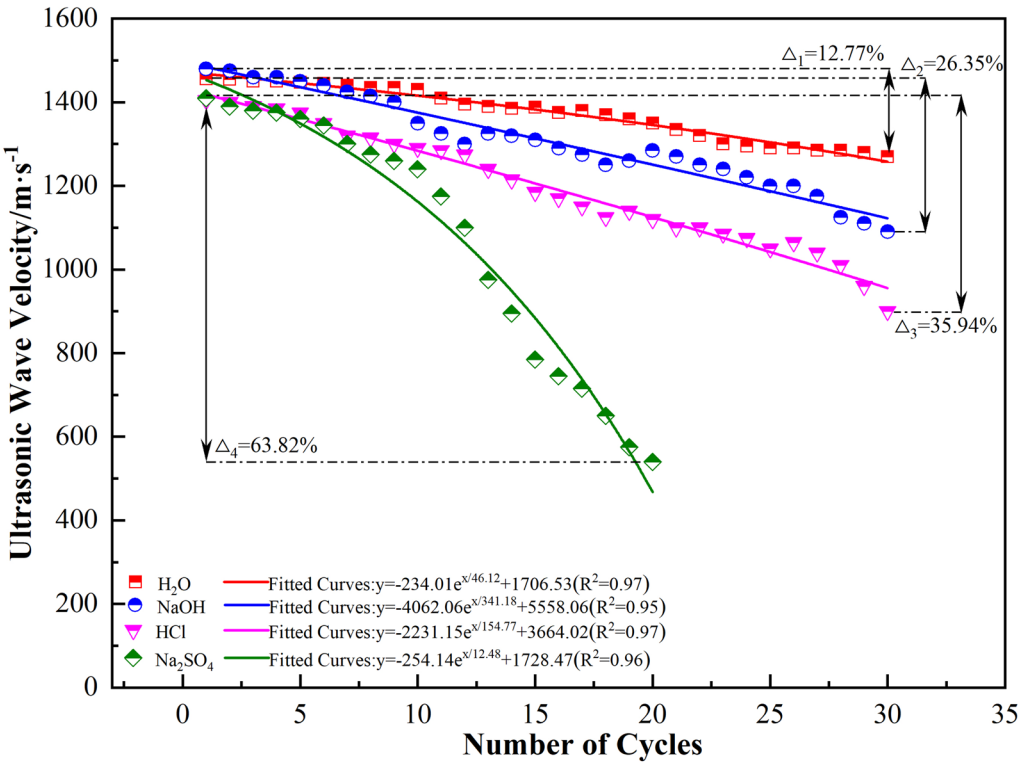

Fig. 11 The relation curve of V_p and number of cycles

loose bonding between layers and numerous microcracks, resulting in lower overall integrity of the samples within the observed field.

Change in Vp

As shown in Fig. 11, under the H_2O cycles, the V_p of the specimen decreases with the increasing number of cycles, albeit slowly. After 30 cycles, the V_p of the specimen decreased from 1456 m/s to 1270 m/s, a reduction of 12.77%. This is mainly due to the increase in internal defects of the specimen under the cyclic effect, resulting in a gradual decrease in V_p. Under the HCl cycles, the V_p of the sample decreases more rapidly. After 30 cycles, the V_p dropped from 1405 m/s to 900 m/s, a decrease of 35.94%. Under the NaOH cycles, the V_p of the sample gradually decreases. After 30 cycles, it dropped from 1480 m/s to 1090 m/s, a decrease of 26.35%. Under the Na_2SO_4 cycles, the V_p of the sample decreases rapidly. After 10 cycles, it dropped from 1410 m/s to 1240 m/s. Continuing the cycle, the sample exhibited a large amount of cracking and damage. By the 20th cycle, the V_p dropped to 540 m/s, and the sample was destroyed, making further testing impossible. Due to the action of water, acid, alkali, and salt, the internal pores and cracks of the sample gradually developed and interconnected, forming larger defects. The density of the sample decreased, leading to varying degrees of decrease in V_p.

Change in mass

Analysis from Fig. 12 shows that under the H_2O cycle, the mass of the sample decreases with the increase in the number of cycles, albeit slowly. After 30 cycles, the mass of the sample decreased from 135.94g to 123.40g, a reduction of 9.22%. This is mainly due to the loosening of surface particles under the environmental erosion cycles, resulting in a reduction in mass. Under the HCl, NaOH, and Na_2SO_4 cycles, the mass of the sample decreases to varying extents. Under the influence of acid and alkali solutions, the mass decreases more rapidly, with reductions of 18.26% and 14.49% respectively after 30 cycles. Under the salt solution, the mass decreases rapidly, with a reduction of 55.32% after 20 cycles, and the sample was destroyed, making further testing impossible. Under the acid, alkali, and salt-dry cycles, the mass loss occurs mainly due to the leaching of calcium binder materials in the sample, leading to the exfoliation of particles.

Change in UCS

Based on the analysis of Fig. 13, it is evident that under the influence of H_2O cycles, the UCS of the ancient brick demonstrates an approximately linear decreasing trend.

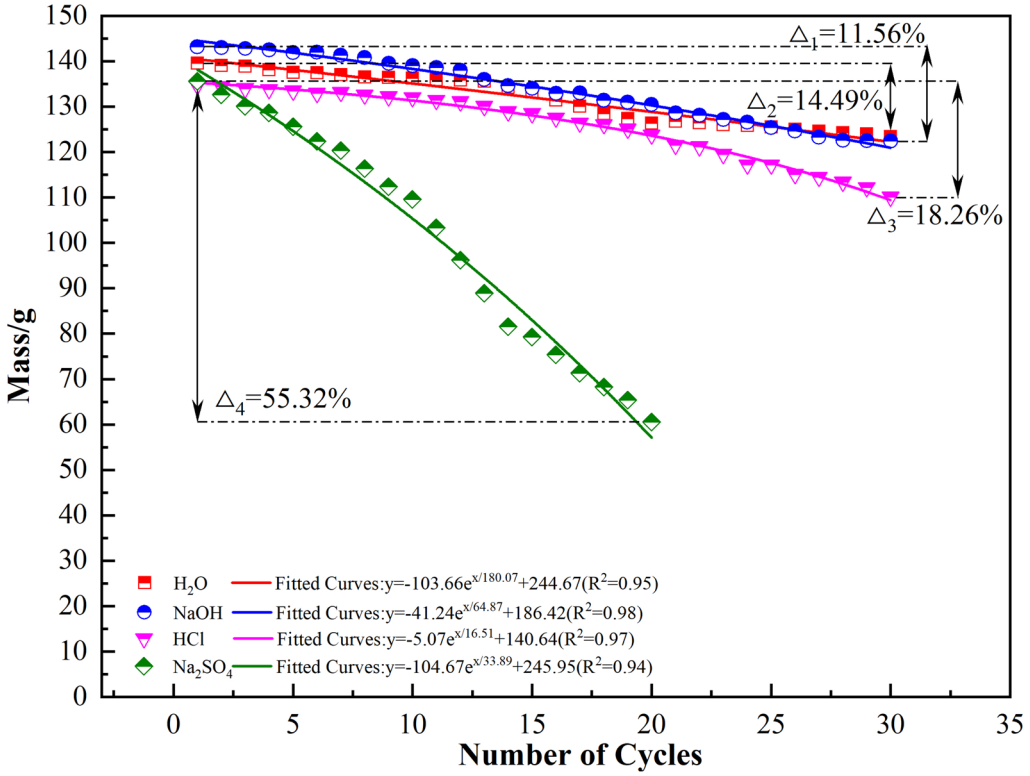

Fig. 12 The relation curve of mass and number of cycles

During the initial 0–20 cycles, the decline is relatively slow. Between 20–30 cycles, the rate of decrease gradually accelerates. After 30 cycles, the unconfined compressive strength of the samples decreases by 16.27%. Under the influence of HCl cycles, the UCS of the samples significantly reduces. In the initial 0–10 cycles, the strength decreases slowly. However, from 10 to 30 cycles, the rate of decline noticeably increases. After 30 cycles, the UCS of the samples decreases by 49.64%. Under NaOH cyclic conditions, the trend in UCS of the samples is similar to that under H_2O cyclic conditions, displaying an approximately linear decrease. The rate of decrease is slower initially but accelerates in the later stages. After 30 cycles, the compressive strength of the samples decreases by 30.28%. Under Na_2SO_4 cyclic conditions, the UCS rapidly declines. After 15 cycles, the compressive strength decreases by 45.96%, and after 20 cycles, the samples are completely deteriorated, making it impossible to test their compressive strength, which considered to be totally lost. These experimental results are consistent with the patterns of V_p and mass change in the samples under environmental erosion conditions, indicating that environmental erosion cycles has varying degrees of impact on the physical and mechanical properties of the specimens.

Change in appearance

From the analysis of Fig. 14(a), it can be inferred that under the influence of H_2O cycles, there are no significant changes in the appearance and microscopic photographs of the samples during the initial 0–20 cycles. After 20 cycles, minor particle detachment is observed on the surface of the ancient bricks. After 30 cycles, the surface particle detachment intensifies, and small pits start to appear.

Analyzing Fig. 14(b) reveals that under HCl cyclic conditions, the impact on the samples is minimal during the first 0–10 cycles. After 20 cycles, minor fine cracks appear on the surface of the samples, which continue to develop as the number of cycles increases. By the end of 30 cycles, these fine cracks have evolved into larger cracks, with maximum widths of 2-3mm, and these cracks run through the entire sample, severely compromising its integrity.

According to the analysis of Fig. 14(c), under NaOH cyclic conditions, there is no noticeable change in the appearance of the samples after 0–20 cycles. After 20 cycles, minor micro-cracks begin to appear on the surface of the samples. Continuing the cyclic process, by the end of 30 cycles, the surface particles of the samples

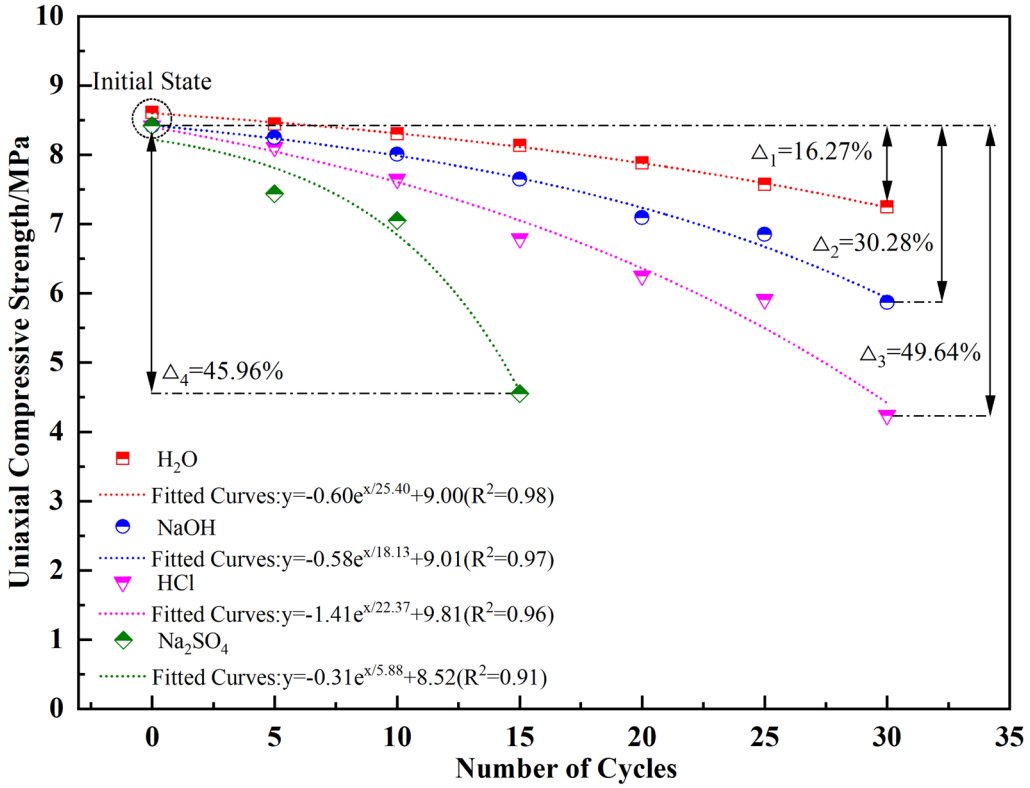

Fig. 13 The relation curve of uniaxial compressive strength and number of cycles

show varying degrees of detachment, and numerous pits are formed.

The analysis of Fig. 14(d) indicates that under Na_2SO_4 cycles, significant changes in the appearance of the samples are evident after 10 cycles, with the emergence of a small amount of crystallization on the surface and minor cracks on the side walls of the samples. After 15 cycles, the crystallization on the surface of the samples increases, and the development of side wall cracks becomes more pronounced. By 20 cycles, crystallization has covered the entire surface of the samples, with extensive particle detachment leading to severe loss of sample mass. The side wall cracks develop through the entire sample, causing it to break completely into two parts, rendering it unsuitable for further testing.

Damage mechanism

The ancient bricks from Wei-Jin tombs exhibited varying degrees of deterioration in performance and microstructural damage under the influence of water (H_2O), acid solution (HCl), alkaline solution (NaOH), and salt solution (Na_2SO_4). The degree of impact, from greatest to least, was observed as follows: $Na_2SO_4 > HCl > NaOH > H_2O$. The reasons for these phenomena are mainly:

(1) As shown in Fig. 15, Na_2SO_4 in a humid environment tends to absorb water and transform into $Na_2SO_4{\cdot}10H_2O$. When the temperature exceeds 32.4°C, $Na_2SO_4{\cdot}10H_2O$ dehydrates to form anhydrous Na_2SO_4, releasing crystal water. Conversely, under temperatures below 32.4°C or humidity above 50%, the anhydrous Na_2SO_4 crystals absorb water and revert to $Na_2SO_4{\cdot}10H_2O$, accompanied by significant volume expansion. This results in repeated expansion and contraction of the samples, leading to noticeable material deterioration [19, 20].

(2) The ancient bricks contain a certain amount of calcite ($CaCO_3$). Under the influence of acid solution (HCl), a chemical reaction occurred between HCl and calcite (Eq. 3). This reaction partially dissolves the surface material of the samples, creating pores and micro-cracks. Continuous action leads to the further development of these micro-crack [13].

$$CaCO_3 + 2HCl \rightarrow CaCl_2 + CO_2 \uparrow + H_2O \quad (3)$$

(3) The ancient bricks contain small amounts of feldspar minerals (albite and orthoclase). Hydrolysis reactions occurred under acidic conditions, which leading to the formation of quartz and clay miner-

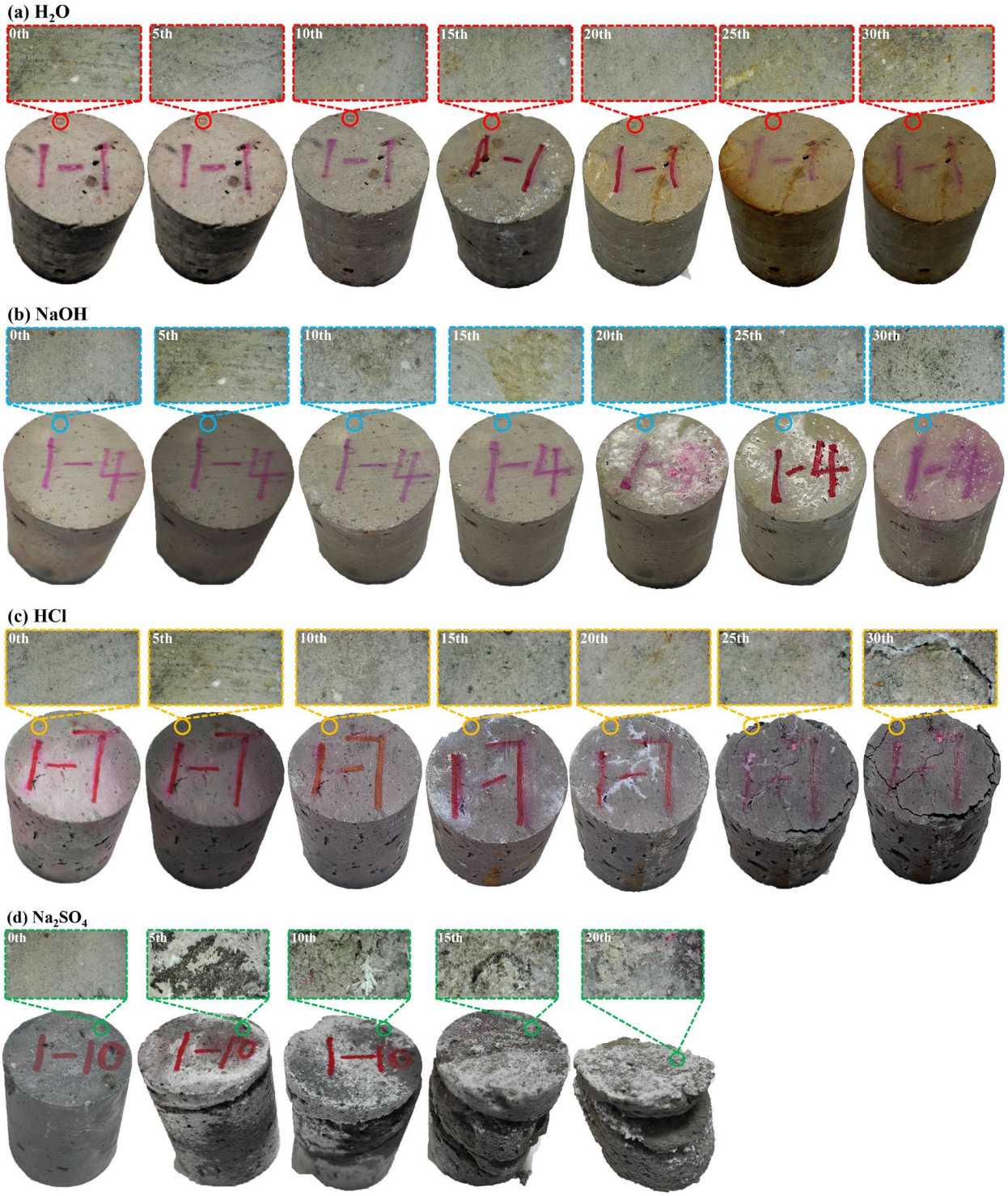

Fig. 14 Appearances and micrographs of samples after different cycles

als (Eq. 4). The original crystalline cemented matrix evolves into a matrix filled with clay, significantly reducing hardness. Although resistant to acid dissolution and chemically stable, these minerals, when combined with water and subjected to external forces, can deform and disperse easily. Therefore,

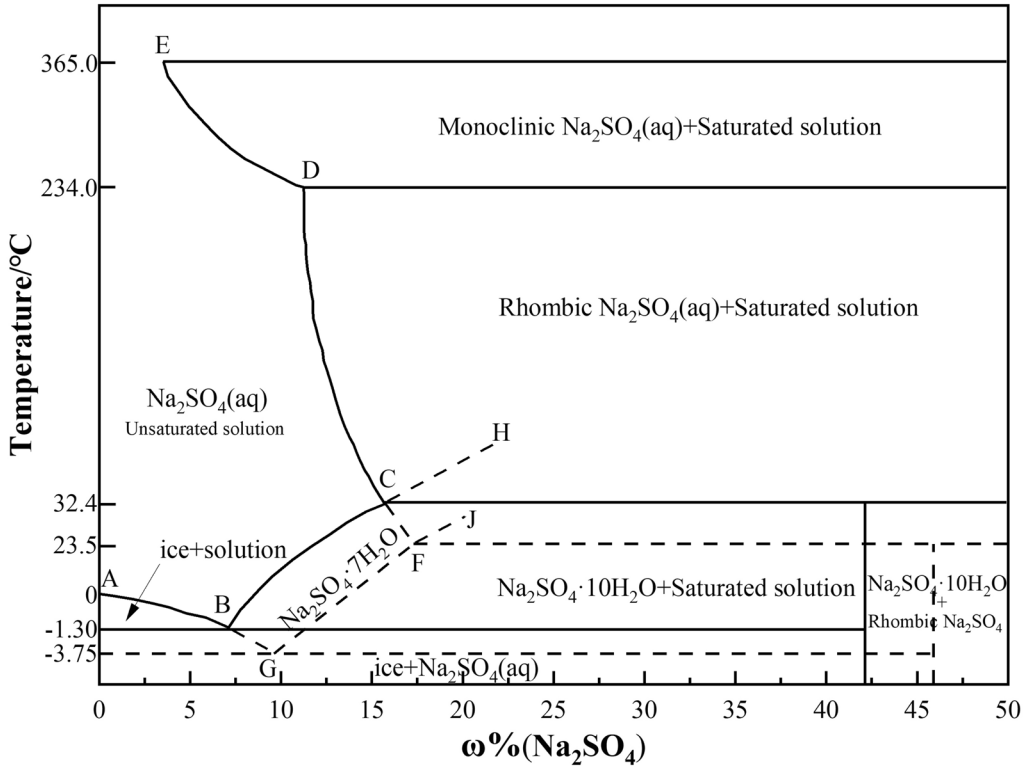

Fig. 15 Phase diagram of Na_2SO_4-H_2O system

the formation of clay minerals considerably reduces the strength of the bricks. Additionally, the good plasticity of clay minerals is also one of the reasons for the formation of cracks in the ancient brick.

$$NaAlSi_3O_8 + 8H_2O \rightarrow Al(OH)_4{}^- + Na^+ + 3H_4SiO_4 \quad (4)$$

Durability analysis of ancient bricks

Due to the long life and high reliability of ancient bricks, it is difficult to collect a sufficient amount of failure data in a short period. Therefore, the traditional probabilistic method is unsuitable for the prediction of the remaining life of ancient brick. As a performance degradation index, the dynamic elastic modulus was used to model the degradation of the relative dynamic elastic modulus and obtain the reliability function of the remaining life of the specimens [21–23].

Due to the low Poisson's ratio, the dynamic elastic modulus of brick (E_d) is calculated by Eq. (5), and the relative dynamic elastic modulus (E_{rd}) is calculated by Eq. (6):

$$E_d = \frac{(1+\upsilon)(1-2\upsilon)\rho V^2}{1-\upsilon} = \frac{(1+\upsilon)(1-2\upsilon)\rho L^2}{(1-\upsilon)t^2} \quad (5)$$

$$E_{rd} = \frac{E_{dt}}{E_{d0}} = \frac{V_t^2}{V_0^2} = \left(\frac{T_0}{T_t}\right)^2 \quad (6)$$

where, ν is Poisson's ratio, ρ is the density of the samples, L is the length of the samples, t is the ultrasonic sound time, E_{dt} is the dynamic elastic modulus at age t, E_{d0} is the dynamic elastic modulus at the initial state, V_t is the ultrasonic wave velocity at age t, V_0 is the ultrasonic wave velocity at the initial state, T_0 is the sound time at the initial state, T_t is the sound time at age t. The E_{rd} value of ancient brick could be calculated by testing the ultrasonic wave velocity after different cycles (V_t) and calculated according to Eq. (6).

Based on field tests, the ancient brick would fail when the E_{rd} decreases by 60%, thus, the durability of bricks in an accelerated test could be tested or calculated by the fitted curve.

The time coefficient (K) is used to analyze the relationship between the durability under natural conditions and that in the accelerated test, which influenced by environmental conditions and matrix structure of samples. The formula of K is as follow:

$$K = \frac{L_{NC}}{L_{AT}} \quad (7)$$

where, L_{AT} is the shortest durability in the accelerated test, and is defined as the minimum number of cycles in each environmental erosion resistance test at which the value of E_{rd} of the sample decreased by 60%. The fitted curves of V_p in each cycle was employed to calculate the value when E_{rd} decreased by 60% due to the long life and high reliability of ancient bricks. Moreover, L_{NC} is the durability under natural conditions. The Wei-Jin tombs in Jiayuguan were excavated for preservation in 1972. According to existing records, the ancient bricks in the tomb chambers were relatively well-preserved initially, with fewer instances of various types of damage. Observations by the cultural relics administration since 2018 have shown an increasing development of diseases such as cracking, exfoliation, and weathering (as shown in Fig. 16), suggesting an L_{NC} value of 46 years for these bricks. The L_{AT} value for the ancient bricks under the conditions of Na_2SO_4 cycle is 20 cycles. Therefore, the time coefficient (K) in this study is calculated to be 2.30.

The durability of the ancient bricks under different conditions can be calculated using the L_{AT} and K values. The results are presented in Table 3. Based on the L_{AT} value under Na_2SO_4 cyclic conditions and observations by the cultural heritage management authorities, the durability of the ancient bricks under H_2O, HCl and NaOH are calculated to be 164.40 years, 156.03 years, and 112.05 years, respectively. These figures are significantly higher than the natural durability of ancient bricks (46 years), indicating that the primary cause of deterioration for these bricks is the salt solution cyclic effect. Future research should focus on the salt damage problem faced by the ancient bricks and develop relevant conservation measures.

Table 3 The results of durability analysis

Cycle type	Fitted curve	L_{AT}/times	L_{NC}/years
H_2O	$y = 1706.53 - 234.01e^{\frac{x}{46.12}}$ ($R^2 = 0.97$)	71.48	164.40
NaOH	$y = 5558.06 - 4062.06e^{\frac{x}{341.18}}$ ($R^2 = 0.95$)	67.84	156.03
HCl	$y = 3664.02 - 2231.15e^{\frac{x}{154.77}}$ ($R^2 = 0.97$)	48.72	112.05
Na_2SO_4	$y = 1728.47 - 254.14e^{\frac{x}{12.48}}$ ($R^2 = 0.96$)	–	46

Conclusion

In this study, the effects of temperature and humidity on the weathering of the ancient bricks are studied by simulating weather changes in an indoor experimental setup, the following conclusions are obtained.

(1) The density of the ancient bricks in Wei-Jin tombs is approximately 1.73 g/cm^3, with an unconfined compressive strength of 8.42 MPa. The ultrasonic longitudinal wave velocity ranges from 1400 to 1500 m/s, and the water absorption rate is 15.21%. The primary mineral compositions include quartz, calcite, gypsum, and a small amount of feldspar minerals. The porosity is 25.71%, and the microscopic morphology is characterized by a lamellar structure that is dense and has few defects.

(2) Cyclic effects have varying degrees of impact on the UCS, V_p, mass, and microstructure of the ancient bricks. The pore size distribution and the porosity significantly increased after HCl and Na_2SO_4 cycles. The degree of impact as follows: $Na_2SO_4 > HCl > NaOH > H_2O$. After 20 cycles of Na_2SO_4 cycles, the sample surfaces are covered with a large amount of crystalline material, and cracks completely penetrate the structure.

Fig. 16 Digital images of Wei-jin tombs at 1972 and 2018

(3) Anhydrous Na_2SO_4, under conditions of temperature below 32.4℃ or humidity above 50%, absorbs water and transforms into $Na_2SO_4{\cdot}10H_2O$, accompanied by significant volume expansion, resulting in noticeable material deterioration of the samples. During the cycling process, reactions also occur in the calcite, feldspar, and other components within the samples, leading to a decrease in the degree of cementation. Pores and fissures gradually increase, even interconnecting to form transverse microcracks.

Author contribution
An Lihong and Zhen Qiao wrote the main manuscript text, Jie Wang and Fengrui prepared figures and tables. All authors reviewed the manuscript.

Funding
This work was supported by Jiayuguan Science and Technology Program (No. 22-40) and Gansu province Science and Technology Program (No. 20YF3FA001).

Availability of data and materials
The datasets used and/or analyzed during the current study are available from the corresponding author on reasonable request.

Declarations

Ethics approval and consent to participate
Not applicable.

Competing interests
The authors declare no competing interests.

Received: 12 December 2023 Accepted: 30 March 2024
Published online: 05 April 2024

References

1. Suhadolnik V. Transmission of Han Pictorial Motifs into the Western Periphery: Fuxi and Nüwa in the Wei-Jin Mural Tombs in the Hexi Corridor. Asian Studies. 2019;7(2):47–86.
2. Li J. A Study of Wei-Jin Ancient Tomb Brick Paintings in Hexi Corridor on China's Silk Road. Int J History Sport. 2013;30(3):232–41.
3. Zhao P, Zhang X, Qin L, et al. Conservation of disappearing traditional manufacturing process for Chinese grey brick: Field survey and laboratory study. Constr Build Mater. 2019;212:531–40.
4. Bruno AW, Gallipoli D, Perlot C. Effect of freezing-thawing cycles on the physical and mechanical properties of fired and unfired earth bricks. J Building Eng. 2022;52: 104501.
5. Uranjek M, Bokan-Bosiljkov V. Influence of freeze–thaw cycles on mechanical properties of historical brick masonry. Constr Build Mater. 2015;84:416–28.
6. Xu J, Xiong W, Guo X, et al. Properties of using excavated soil waste as fine and coarse aggregates in unfired clay bricks after dry-wet cycles. Case Stud Const Mater. 2022;17: e01471.
7. Xia C, Liu D, Kong Z, et al. Spatial and temporal changes in microclimate affect disease distribution in two ancient tombs of Southern Tang Dynasty. Heliyon. 2023;9(7): e18054.
8. Fan Y, Song S, Huang J, et al. Study on weathering mechanism of masonry bricks of ancient temples in Shanxi province using Dingxiang Hongfu temple masonry brick. Constr Build Mater. 2019;222:500–10.
9. Lu K, Li F, Pan J, et al. Using electrical resistivity tomography and surface nuclear magnetic resonance to investigate cultural relic preservation in Leitai, China. Eng Geol. 2021;285: 106042.
10. Xia Q, Yi T, Li Y, et al. Analysis of Chinese ancient brick masonry characteristics under uniaxial compression fatigue loading. Constr Build Mater. 2023;392: 131874.
11. Liu W, He D, Geng T, et al. Comparative life cycle assessment of cement, sintered bricks and non-sintered bricks manufacturing using water-based drilling cuttings from shale gas production in the Sichuan Basin, China. J Environ Manage. 2022;314: 115135.
12. Raza IA, Maaze R, et al. Comparative life cycle assessment of recycled soil-stabilized bricks and traditional bricks. Materials Today Proc. 2023;80:532–7.
13. Arnold A. Rising damp and saline minerals [C]. Deterioration & Preservation of Stone Objects Fourth International Congress Proceedings, 1982.
14. Steiger M. Distribution of salt mixtures in a sandstone monument: sources, transport and crystallization properties [C]. Protection and Conservation of the European Cultural Heritage. Research Report 4. Bari: European Commission, 1996. p. 241.
15. Steiger M, Behlen A, Neumann H, et al. Sea salt in historic buildings: deposition, transport and accumulation [C]. Fourth International Symposium on the Conservation of Monuments in the Mediterranean Basin. Rhodes/Athens: Technical Chamber of Greece, 1997. p. 325.
16. Arnold A, Zehnder K. Decay of stony materials by salts on humid atmosphere [C]. Sixth International Congress on Deterioration & Conservation of Stone Torun September Proceedings, 1988.
17. Zhao P, Zhang X, Qin L, et al. Conservation of disappearing traditional manufacturing process for Chinese grey brick: Field survey and laboratory study. Constr Build Mater. 2019;212(10):531–40.
18. Tite M. Determination of the Firing temperature of ancient ceramics by measurement of thermal expansion: a reassessment. Archaeometry. 1969;11(1):131–43.
19. Steiger M, Asmussen S. Crystallization of sodium sulfate phases in porous materials: The phase diagram Na_2SO_4—H_2O and the generation of stress. Geochim Cosmochim Acta. 2008;72(17):4291–306.
20. Bharmoria P, Gehlot PS, Gupta H. Temperature dependent solubility transition of Na_2SO_4 in water and the effect of NaCl therein: solution structures and salt water dynamics. J Phys Chem B. 2014;118(44):12734–42.
21. Gong W, Wang N, Zhang N, et al. Water resistance and a comprehensive evaluation model of magnesium oxychloride cement concrete based on Taguchi and entropy weight method. Constr Build Mater. 2020;260(9): 119817.
22. Cao H, Zhao LF, Lu CG, et al. Degradation Resistance and Reliability Analysis of Recycled Aggregate Concrete in a Sulfate Environment[J]. Adv Mater Sci Eng. 2020;2020(5):1–11.
23. Qiao Z, Ding Z, Wang J, et al. Enhanced mechanical properties and environmental erosion resistance with metakaolin in a kind of Chinese traditional Lime-based mortar. Constr Build Mater. 2022;317: 126110.

Publisher's Note